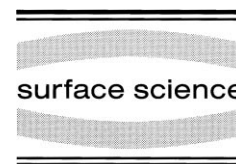




ELSEVIER

Surface Science 408 (1998) 1–20



# Benzene adsorbed on Cu(110): theoretical X-ray absorption, emission and shake calculations

L.G.M. Pettersson<sup>a</sup>, H. Ågren<sup>b,\*</sup>, Y. Luo<sup>a,b,c</sup>, L. Triguero<sup>a</sup>

<sup>a</sup> FYSIKUM, University of Stockholm, Box 6730, 11385 Stockholm, Sweden

<sup>b</sup> Institute of Physics and Measurement Technology, Linköping University, 58183, Linköping, Sweden

<sup>c</sup> Department of Chemistry, University of Copenhagen, 2100 Copenhagen, O, Denmark

Received 16 July 1997; accepted for publication 13 January 1998

## Abstract

Geometry optimization of benzene on Cu(110) results in two possible stable chemisorbed structures; an inverted boat, quinoid, conformation which probably is produced via a reaction involving a barrier, and a planar carbon ring structure with the hydrogens flipping upwards, which is only 4 kcal mol<sup>-1</sup> less stable. We carry out quantum chemical calculations of X-ray spectroscopies for benzene chemisorbed on Cu(110) with the intention to demonstrate the possible relations between internal adsorbate restructuring and the appearance of X-ray spectra; X-ray emission-, -absorption - and -photoelectron shake spectra. The two predicted optimum adsorbate structures are shown to have particular implications for the character of the spectra, something that is discussed in light of recent experimental measurements on C<sub>6</sub>H<sub>6</sub>/Cu(110) (Nilsson et al., to be published) and on chemisorbed benzene in general. It is found that, while planar benzene or benzene with the hydrogen bent upwards is associated with only one  $\pi^*$  resonance, boat formed benzene is associated with three. The bonding to the surface induces extra  $\pi$  character in the discrete NEXAFS (near-edge X-ray absorption fine-structure) spectra of both conformations. In the case of X-ray emission (XES) the restructuring gives rise to  $\sigma$ - $\pi$  symmetry breaking with an altered orientational dependence for the emitted X-ray photons. Comparison with experiment indicates that both structures can describe the orientational dependence in the XES spectra, while the recorded NEXAFS spectrum for C<sub>6</sub>H<sub>6</sub>/Cu(110) is better reproduced by the less distorted structure. In the case of shake-up it is found that the salient features appear too complex to be used for diagnostization of internal adsorbate restructuring. © 1998 Elsevier Science B.V. All rights reserved.

**Keywords:** Ab initio quantum chemical methods and calculations; Adatoms; Aromatics; Copper; Density functional calculations; Near edge extended X-ray absorption fine structure (NEXAFS); Soft X-ray photoelectron spectroscopy; X-ray emission

## 1. Introduction

In the present work we bring up one particular aspect of structure–property relationships for surface adsorbates, namely the role of internal restructuring of the adsorbate for the appearance of X-ray spectra; X-ray emission (XES), X-ray absorption (XAS) and X-ray core electron photoemission [X-ray photon spectroscopy (XPS)

shake-up] spectra. This is accomplished by optimization of the electronic and geometric structures of a cluster model, C<sub>6</sub>H<sub>6</sub>/Cu<sub>13</sub>, of benzene adsorption on Cu(110) and by calculations that predict X-ray spectra of this model. Benzene on copper constitutes a prototype system for hydrocarbon adsorption on surfaces, and for the general role of  $\pi$  versus  $\sigma$  bonding for this adsorption. It also represents a nice example when adsorbate restructuring might be anticipated, but where it is not yet proven so.

The bonding of unsaturated hydrocarbons to

\* Corresponding author. Fax: (+46) 26 13137568;  
e-mail: agren@ifm.liu.se

transition metal surfaces usually implies strong distortions of the molecular structure with concomitant loss of bond order. Acetylene and ethylene chemisorption on copper surfaces are thus typically associated with C–C bond-elongations of the order of 0.1–0.2 Å in combination with a bending up of the hydrogens away from the substrate. These changes in the internal structure of, for example, acetylene and ethylene upon adsorption are normally discussed in the framework of a  $\pi$ -donation– $\pi^*$ -backdonation picture [1,2], but a more detailed understanding may be obtained by considering the bond-preparation of the adsorbate through an internal spin-uncoupling [3]. For acetylene this implies that the gas phase excited triplet state should be considered, while for ethylene the eclipsed structure of the gas phase triplet state becomes involved in the bonding. The latter is actually a transition state in the gas phase, but becomes stabilized through the interaction with the substrate [3]. For each of these systems a large excitation energy is required to reach the bonding electronic structure (bond preparation), but the energy gain from individual carbon–metal bond formation is sufficiently large to compensate this and the result is a small net chemisorption energy coupled with large geometrical distortions.

In applying the picture of bond-preparation through spin-uncoupling to the more complex benzene molecule one has two excited triplet states to consider for the gas phase system: a quinoid structure with two short C–C distances and the remaining four elongated, and the antiquinoid structure which has the opposite distortions. The gas phase quinoid structure furthermore shows a slight distortion into an inverted boat conformation with a slight bending up of the hydrogens; this structure is bond-prepared for bonding at the two opposite carbons (*para*-position) and is the most favorable structure that actually results from optimization of benzene on the Cu(110) surface [3]. This type of structure has also been noted experimentally for benzene chemisorption on several substrates, but the error bars in the structural determinations are such that the distortions from planarity of the ring system cannot be considered statistically significant [4]. A second possible structure for chemisorbed benzene is a structure in

which the planarity of the carbon ring is maintained, but for which the hydrogen atoms are bent up from the surface; we find this structure to be 4 kcal mol<sup>-1</sup> less stable than the inverted boat conformation. One way to aid in determining the actual structure could then be to compute theoretical XAS emission and shake spectra for various structures; from planar benzene in the gas phase, benzene with just the hydrogens bending up, the optimized inverted boat structure in the gas phase with both hydrogen bending and carbon backbone distortion, and finally the optimized structures interacting with the substrate. This may enable a characterization of the origin of the different features detected using the various spectroscopies and a finger-printing of effects on the spectra from different geometrical modifications. In the following we describe results for free benzene, and for the two chemisorbed systems. We compare the results with relevant available XES, NEXAFS and shake-up measurements for benzene adsorbed on surfaces, and for the Cu(110) surface in particular.

## 2. Method and calculations

We employ well-established computational techniques: SCF (self-consistent field) and STEX (static exchange) calculations of spectra and the density functional method for the geometry optimization. The SCF and STEX techniques have been described in previous papers [5,6], in particular with respect to the use of integral-direct and basis set augmentation techniques that enable the calculations of “large” species close to basis set saturation. The description of the cluster modelling, including the use of ECPs (effective core potentials) for calculations of surface adsorbate spectra, can be found in Refs. [7,8]. We refer to these papers also for the description of special features of the implementation, and to some rigorous tests of the method with respect to sum rules and gauge dependency. The geometry optimization employs all-electron density functional theory (DFT) including gradient corrections [9,10]; the spectral calculations have employed cluster atoms described by one-electron ECPs [11] in which the core (includ-

ing the 3d-shell) is described by a static potential, which includes the effects of relaxation and polarization of the 3d-orbitals, but which only treats the 4sp-valence electrons explicitly. The basis set used is a (4s 1p) primitive basis contracted to [2s 1p] [11], as extensively tested for general applications [12] including NEXAFS [7]. For adsorbed and free benzene we used a TZPD (triple zeta plus polarizing and diffuse functions) basis set [13]. In addition, the molecular basis set was augmented with a large (141 functions) diffuse basis centred on the centre with the core hole. This basis set was generated by adding 19s, 19p and 19d functions with exponents obtained by an even-tempered scaling,  $\alpha_n = \alpha_0 \beta^{-n}$ , with  $\alpha_0 = 1.238 a_0^{-2}$  and  $\beta = 1.4$ ; the smallest exponent used was  $0.0029 a_0^{-2}$ . The direct SCF program DISCO [14] including its modification for STEX calculations [5] is used as the underlying electronic structure code. The static exchange approximation implies neglect of the relaxation of the molecular ion core in the presence of the excited electron. This approximation is very accurate for the Rydberg states, but gives errors in the computed  $\pi^*$  excitation energies of benzene of the order of 1 eV [15]. This excitation energy can be computed separately and the  $\pi^*$  peak position shifted to include the relaxation; this has been done for all the absorption spectra presented in the present work. The cross-sections in the continuum are obtained by applying the Stieltjes imaging procedure to the set of eigenvectors and eigenvalues obtained from the STEX calculation [5]. For the geometry optimization the deMon code [16,17] was used with triple- $\zeta$  plus polarization quality basis sets (d on carbon, p on hydrogen) to describe the adsorbate and the Wachters [18] all-electron basis set for the 13 all-electron coppers in the cluster model [3]. The optimization was performed using analytical energy gradients and optimizing the positions of all atoms of the adsorbate, while keeping the substrate atoms fixed; the two different final structures were obtained by assuming different starting geometries in the optimization.

Without second-derivative information the determination of the character of the obtained structures becomes uncertain. We feel, however, quite confident of the correctness of the solutions

obtained in the present work, both for the “boat” distorted, quinoid structure and the less distorted “H-flip” structure. The quinoid structure is the lowest energy state found, with the “H-flip” structure some  $4 \text{ kcal mol}^{-1}$  higher in energy. Both structures correspond to experimentally known, ground or excited, molecular states which must exist also on the substrate. The more difficult question about possible effects of substrate relaxation, we cannot address in the present work since this would require substantially larger cluster models. However, we do not expect large effects since, even though the carbon backbone is distorted in the quinoid structure, no particular strain on the molecule is involved; the adsorbate structure, including carbon backbone distortion, is very close to the gas phase optimum structure for this particular molecular state.

### 3. Results and discussion

#### 3.1. Cluster geometry

The two lowest-energy optimized structures, the “boat” and “H-flip” structures of  $\text{C}_6\text{H}_6$  on the  $\text{Cu}_{13}$  cluster model of the Cu(110) substrate are displayed in side- and top views in Fig. 1, with the optimized bond lengths given in Table 1 [3]. The cluster includes two layers of copper atoms and is sufficiently large to “cover” the benzene molecule. As indicated by the figure, the first (“boat”) adsorbate structure has  $\text{C}_{2v}$  symmetry with the carbon ring bent in an inverse boat-like form and with the hydrogen atoms flipped upwards; this structure corresponds to the quinoid structure of the gas phase excited triplet state. Experimental data, for example, NEXAFS, low energy electron diffraction (LEED) and PhD data, often indicate a significant prolongation of C–C distances and a reduced bond order upon adsorption of unsaturated hydrocarbons on copper surfaces, for instance ethylene and acetylene prolong their C–C bonds by 0.10 and 0.26 Å, respectively, when adsorbed on a Cu(111) surface [4]. There are indications that the same happens with benzene; both the resonance structure with equal C–C bond lengths and the planarity of the molecule might be broken upon

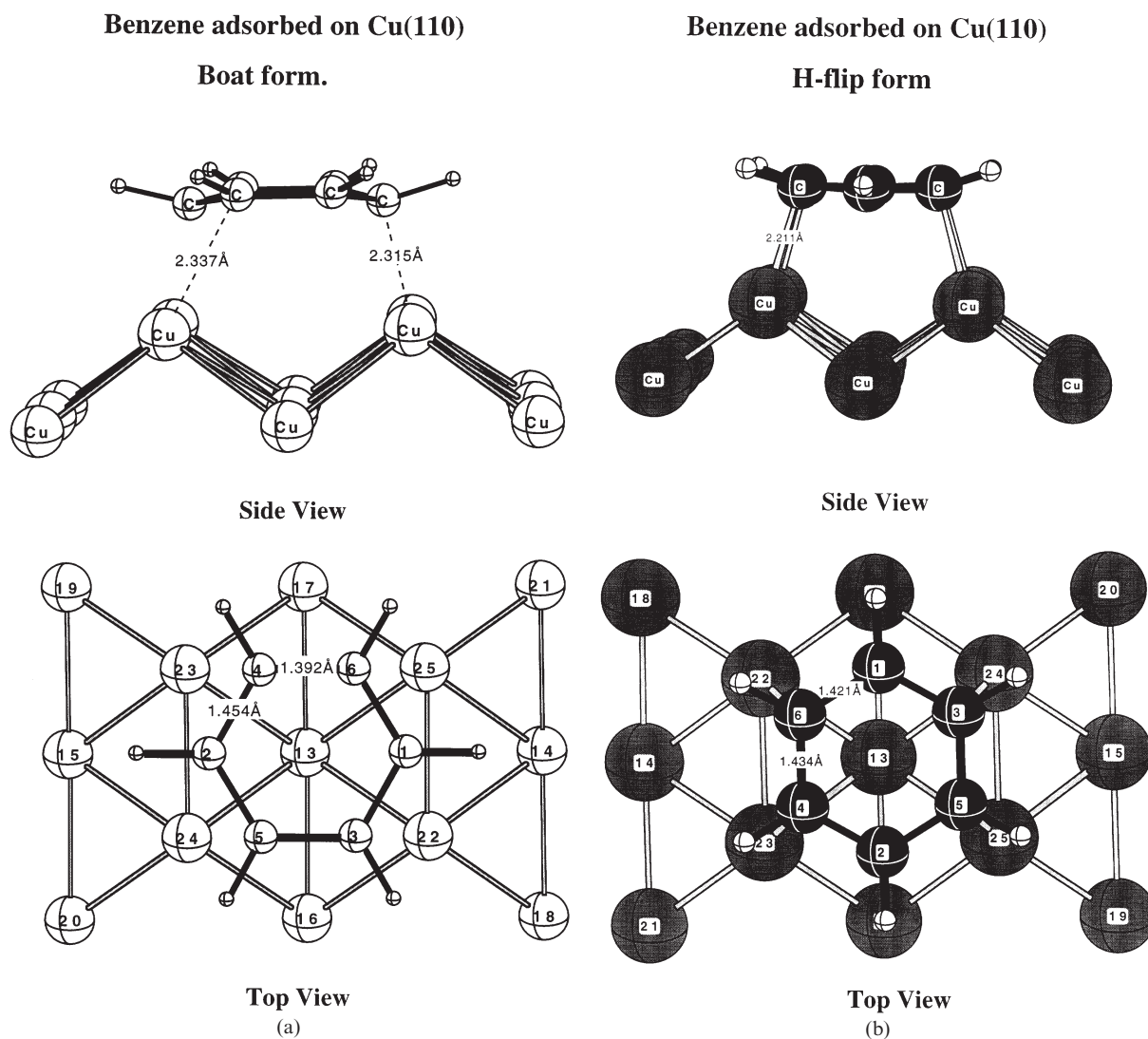


Fig. 1. Structures of the  $C_6H_6/Cu_{13}$  cluster. Side (a) and top (b) views of the quinoid boat structure and side (c) and top (d) views of the less distorted H-flip structure.

adsorption. However, according to Ref. [4], none of the deviations from planarity indicated by fitting to spectra are statistically significant; in fact, Held et al. [19] find for  $C_6H_6$  on Ni(111) that the substrate reconstructs somewhat rather than that the planarity of the ring system breaks. From this outset it is interesting to note that the present simulations do predict both a C–C bond elongation and a breaking of the carbon back-bone planarity for the “boat” structure; two C–C bonds

remain as in the gas phase, while the other four are elongated by  $0.05 \text{ \AA}$  combined with an angle of carbon plane bending of  $7.4^\circ$  and bending up of the hydrogens by  $17.5^\circ$ . For the less distorted “H-flip” structure the C–C bond lengths show a small and symmetrical elongation by  $0.02\text{--}0.03 \text{ \AA}$ , four of the hydrogens bend up by  $17.6^\circ$  while the two hydrogens in *para*-position show a smaller,  $5.3^\circ$ , degree of bending against the plane of the ring.

Table 1  
Optimized geometry (distances in Å and angles in degrees) and computed chemisorption energy  $D_e$  (kcal mol<sup>-1</sup>) for C<sub>6</sub>H<sub>6</sub>/Cu<sub>13</sub> all-electron cluster (the numbering of the atoms corresponds to that in Fig. 1)

Property	Gas phase	Chemisorbed geometry	
	Singlet	Boat form (110)	H-flip form (110)
C <sub>1</sub> –C <sub>6</sub>	1.40 (1.397) <sup>a</sup>	1.45	1.42
C <sub>6</sub> –C <sub>4</sub>	1.40 (1.397) <sup>a</sup>	1.39	1.43
C–H	1.08 (1.084) <sup>a</sup>	1.09	1.09
Cu <sub>23</sub> –C <sub>4</sub>	–	2.31	2.21
Cu <sub>22</sub> –C <sub>1</sub>	–	2.34	–
Z <sup>C<sub>1</sub></sup> <sup>b</sup>	–	1.89	2.05
Z <sup>C<sub>6</sub></sup> <sup>c</sup>	–	2.05	2.05
C <sub>1</sub> C <sub>6</sub> C <sub>4</sub>	120.0	120.7	120.2
C <sub>3</sub> C <sub>1</sub> C <sub>6</sub>	120.0	117.0	119.5
C <sub>4</sub> C <sub>6</sub> C <sub>1</sub> C <sub>3</sub>	0.0	7.4	0.4
H <sub>7</sub> C <sub>1</sub> C <sub>6</sub> C <sub>4</sub>	0.0	17.5	5.3
H above ring	0.0	17.5	17.6
$D_e^d$	–	18	14

<sup>a</sup>Experimental data from Ref. [58].

<sup>b</sup>Z<sup>C<sub>1</sub></sup> = C<sub>1</sub> height above the surface.

<sup>c</sup>Z<sup>C<sub>6</sub></sup> = C<sub>6</sub> height above the surface.

The geometry optimized for the benzene–copper cluster with a distortion of the carbon backbone into an inverted boat form with a quinoid structure, corresponds to one of the two experimentally known gas phase triplet states of free benzene. This infers that the chemical activation of surface adsorption includes a spin uncoupling in the benzene adsorbate, which corresponds to the excitation to the triplet state; in combination with the corresponding spin-uncoupling on the substrate (e.g. the cluster) the overall low-spin coupling of the combined system is still maintained. In spite of the large stability of the ground state benzene molecule we find a high structural flexibility in the excited triplet state; the energy required to move the molecule from the gas phase optimal quinoid structure to that actually optimized on the cluster is very low (8 kcal mol<sup>-1</sup>). The computed 98 kcal mol<sup>-1</sup> excitation energy to the triplet quinoid structure, can be compared with the (computed) chemisorption energy of 18 kcal mol<sup>-1</sup> which indicates a C–Cu bond energy of 58 kcal mol<sup>-1</sup> (assuming two such bonds). The

undistorted, “H-flip”, structure cannot form direct covalent carbon–copper bonds to the substrate and must instead interact through polarization of the  $\pi$ -system; the computed bondstrength in this interaction is 14 kcal mol<sup>-1</sup> [3]. Assuming that this bonding mechanism exists also for the distorted quinoid structure we must remove this binding energy contribution from the total chemisorption energy before assigning a per-covalent-bond energy in the case of the distorted structure. The per-bond energy then becomes 51 kcal mol<sup>-1</sup>, which complies very well with individual bond strengths for other 4 carbons adsorbed on Cu(110); for example, the computed average C–Cu bond energy of acetylene and ethylene on Cu(100), Cu(110) and Cu(111) is found to be 493 kcal mol<sup>-1</sup> [3].

### 3.2. XAS spectra

#### 3.2.1. NEXAFS of free benzene

No consensus has been reached on the correct assignment of the NEXAFS spectrum of benzene although it has been studied on many occasions experimentally [20–22] as well as theoretically [21, 23–25]. The spectrum shows two main discrete and two main continuous features on a coarse scale. Because of the equivalence of all carbon–carbon bonds the diatom building block picture predicts, however, only one  $\pi^*$  and only one  $\sigma^*$  type resonance [26]. The present calculations, identical with those given in Ref. [25], seem to corroborate with this picture, thus contradicting the original assignment of the four main features as two  $\pi^*$  and two  $\sigma^*$  resonances [21], see Fig. 2. These calculations (as those in Ref. [24]), predict the weaker second discrete band to be of  $\sigma$  symmetry, actually containing three closely split  $\sigma$  transitions (in fair agreement with K-shell electron energy loss [20] and the most recent XAS data [27]). The calculations place the next transition close to the IP. The lowest, C 1s– $\pi^*$ , transition is excitonic and collects much of the total oscillator strength, implying a weakened remainder of discrete transitions. It seems to fingerprint phenyl rings in polymer environments very well [15, 25].

The intensity distribution of the discrete features is well recapitulated, although excitation energies

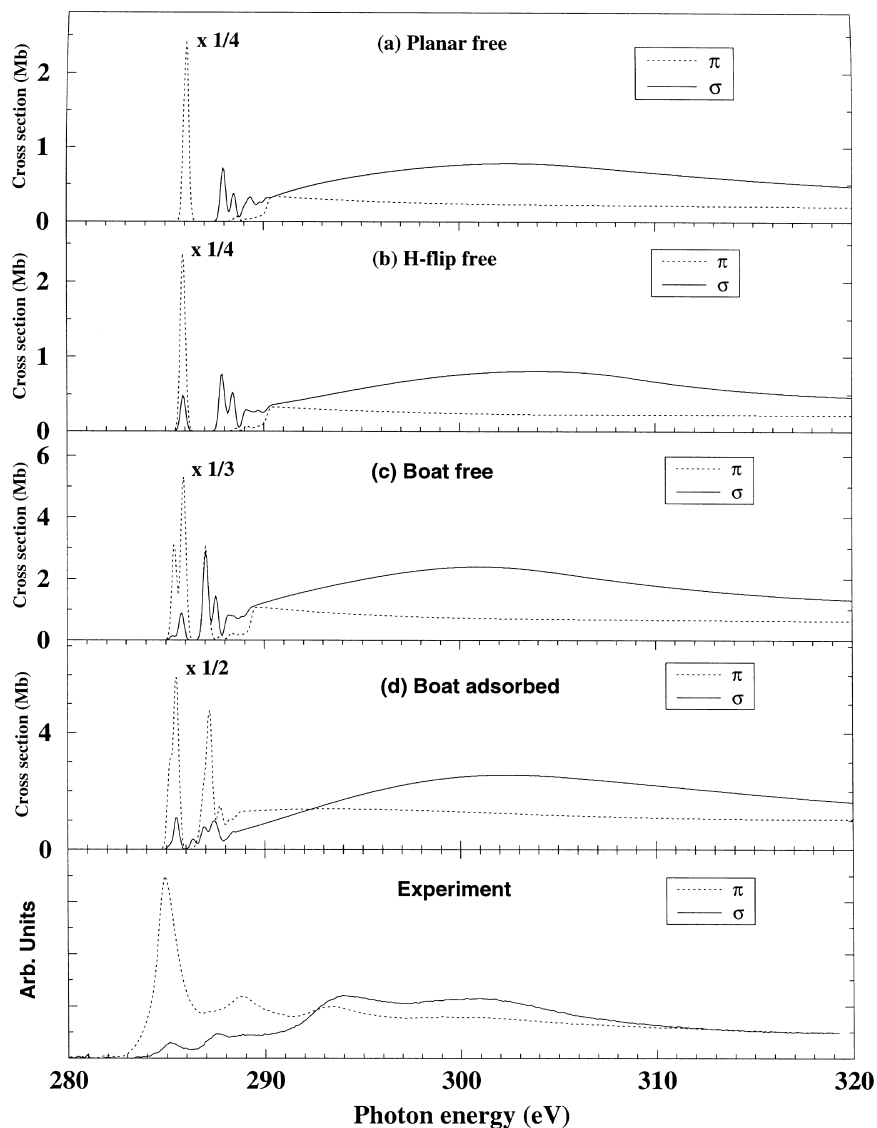


Fig. 2. Simulated XAS spectra of benzene. (a) Planar free benzene in gas phase geometry. Spectral lines are convoluted with gaussians with  $\text{FWHM}=0.3$  eV. (b) Free benzene with hydrogen flipping upwards. (c) Free benzene with distorted boat form geometry. (d) Surface adsorbed benzene with distorted boat form geometry.

are somewhat compressed and shifted upwards on an absolute scale, due to the typical residual screening effect for valence  $\pi^*$  levels unaccounted for by STEEX, but which can be included through an explicit  $\Delta\text{SCF}$  calculation of the excitation energy; this has been done for the  $\pi^*$  resonance, which has the largest relaxation effect (1 eV). An assignment of the first resonance seen in the experiment

as due to multi-electron excitations associated to the very strong  $\pi^*e_{2u}$  resonance has been argued for, see Ref. [25].

### 3.2.2. Symmetry analysis of benzene NEXAFS spectra

It is relevant to analyse the NEXAFS spectra in terms of symmetry reduction induced by core hole

excitation, by corruption of the benzene skeleton ring, or by the surface orientation. For the  $C_6H_6/Cu(110)$  system the analysis then concerns the  $D_{6h}$ ,  $C_{2v}$  and  $C_s$  symmetries. Indication of symmetry breaking of the first core-excited  $e_{2u}$  state in benzene was given through high-resolved NEXAFS spectra showing vibrational distortions [27,28]. On grounds of the magnitude of the frequencies this vibrational distortion was assigned to non-totally symmetric modes [28]. Full geometry optimization of the core excited states also indicate such a pseudo Jahn–Teller instability towards an optimum nuclear configuration of  $C_{2v}$  symmetry [29]. A further corruption to a boat form of the benzene ring then gives  $C_s$  symmetry, and the extra  $\pi$  peak in boat-form benzene can be understood by considering the orbital symmetries of planar and boat-form benzene. In the  $D_{6h}$  point group the doubly degenerate  $e_{2u}$  orbital has one component localizing mainly on the four carbons, and one component localizing on the other two. This  $e_{2u}$  orbital splits into two orbitals,  $b_1$  and  $a_2$ , in the  $C_{2v}$  point group of the boat form. Adopting the symmetry-broken representation for core excitation the core orbital is always totally symmetric. Therefore, in the case of planar benzene

$$1s_a \rightarrow b_1 \pi \text{ transition} \quad (1)$$

$$1s_a \rightarrow a_2 \text{ forbidden} \quad (2)$$

In the case of distorted benzene (Fig. 1), the symmetry of the molecular frame is lowered to  $C_{2v}$ , with the six carbon atoms splitting into two groups with either two (C1) or four (C3) symmetry-equivalent centres. In addition, the degeneracy of the ground state  $b_1$  and  $a_2$  orbitals is lifted. Upon the core excitation, the electronic symmetry of the molecule might be further broken, depending on which core orbital is excited. If the excitation is at one of the C1 carbons, the symmetry of the molecule is broken into  $C_s$  symmetry, and the two unoccupied orbitals,  $b_1$  and  $a_2$ , in the  $C_{2v}$  frame, will transform as  $a'$  and  $a''$  in the new  $C_1$  frame, and as  $T_z$  and  $T_x$ ,  $T_y$ , respectively, in the cartesian frame (in this paper called “ $\pi$ ” and “ $\sigma$ ”). One then has to consider the transitions

$$1s_a \rightarrow a' \pi \text{ level} \quad (3)$$

$$1s_a \rightarrow a'' \sigma \text{ level} \quad (4)$$

which only provide one  $\pi^*$  resonance in the absorption spectrum, but an “extra”  $\sigma$  transition further up (see Fig. 3a). By contrast, if the excited core orbital resides at C3, the symmetry of the molecule is further broken into  $C_1$  upon core excitation and both  $\pi^*$  orbitals will be of a symmetry. The transitions can then be illustrated as

$$1s_a \rightarrow a \pi + \sigma \text{ mixed level} \quad (5)$$

$$1s_a \rightarrow a \pi + \sigma \text{ mixed level} \quad (6)$$

that is, there will be two  $\pi^*$  peaks in the absorption spectrum.

### 3.2.3. NEXAFS of boat-form benzene

The symmetry analysis given above indicates that, in contrast to planar benzene, which has only one  $\pi^*$  resonance, boat-form benzene has three. For the  $C_6H_6/Cu_{13}$  cluster the simulations predict a splitting between the first C1 and C3 resonances of 0.3 eV, which is significantly lower than the predicted XPS shift of 1.0 eV as is typical for systems with self-screening levels [26,30]. The remainder of the discrete NEXAFS spectrum of the boat-form is, however, chemically shifted in that the “top” four equivalent carbon sites show a second strong  $\pi^*$  transition, while the two equivalent carbon atoms closer to the substrate lack this transition, and show in fact a spectrum that is quite like free benzene, see Fig. 3. The splitting between the two C3 resonances is 1.6 eV according to the present calculations. Fig. 2c shows that, after convolution, the spectrum of boat-form benzene reinforces a picture with two strong bands in the discrete part and one, a  $\sigma^*$  shape resonance, in the continuum. The spectra of free benzene in the corrupted surface adsorbed boat form show some intensity of a second  $\pi$  peak; the presence of the surface – and thus the surface bonds – enforces a purer character of the peak, compare Fig. 2c and d. (It is relevant here to note that the double band structure in the discrete NEXAFS spectra of *p*-benzoquinone and related species is associated to the chemical shifts of the  $e_{2u}$   $\pi^*$  transition due to the substituents as discussed in Ref. [31]). A closer inspection of Fig. 3a indicates that also the C1 carbons provide  $\sigma$  contribution to the first peak at ca 285 eV, and that the transitions referring to

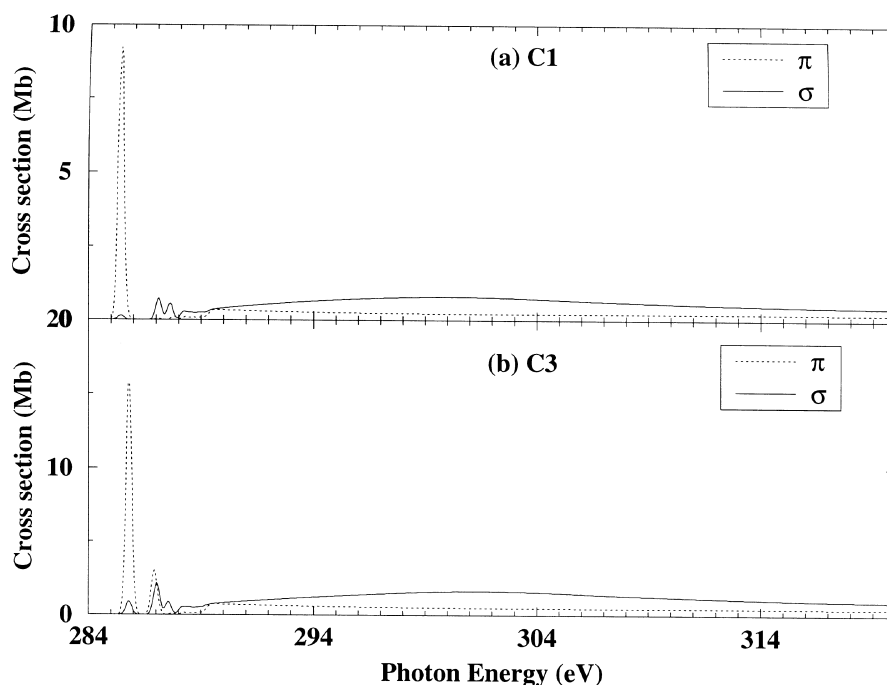


Fig. 3. Simulated XAS spectra of free benzene in boat form. Spectral lines are convoluted with gaussians with FWHM=0.3 eV. (a) Excitation in C1 atom. (b) Excitation in C3 atom.

both carbon types reside in the intermediate region. The continuum  $\sigma^*$  resonance is furthermore differently perturbed upon adsorption depending on the chemical site.

#### 3.2.4. NEXAFS of H-flip benzene

The actual occurrence of the inverted-boat structure is not uncontroversial; XAS measurements of benzene on Cu(110) reported in Ref. [32] indicate a second  $\pi^*$  peak 3.9 eV up, see Fig. 4, while measurements of benzene on Ni(100) indicate secondary character much closer to the main peak [32]. It seems that the spectrum generated by the “H-flip” structure is closer to experiment both with respect to energy and intensity, see Fig. 4. It is therefore relevant to use the experimental comparison with the H-flip results to analyse the origin of the observed structures. Considering the main  $e_{2u}$  285 eV peak we note that the simulations accord with experiment in that no “onset” structure is predicted and in that a slight  $\sigma$  contribution is given to this peak. The presence of this contribution has actually been used to argue for both tilted

[33] and rehybridized [32] (“H-flip”) configurations. The simulations predict such a feature also for free benzene (see “H-flip” free on panel 3 of Fig. 2) which suggests that this feature has a lot to do with the internal restructuring of the adsorbate. The next debated feature is centred at 289 eV in the experimental spectrum [32], and is assigned as mainly due to state(s) with  $\pi$  character. Indeed two  $\pi$  states turn up in this region from the “H-flip” adsorbate simulations, which, when convoluted with the nearby rather sharp  $\pi$ -like onset of the continuum, can explain the experimental finding well. Interestingly, neither “planar free” nor “H-flip free” benzene predicts  $\pi$  intensity in this region (Fig. 2; only three  $\sigma$  peaks, as commented in Section 3.2.1), so this feature must be attributed to the bonding with the surface. The simulation for the adsorbed species predicts a reminiscence of  $\sigma$  intensity also in this spectral region.

#### 3.2.5. Comments on NEXAFS spectra of surface adsorbed benzene

The dependence of the XAS cross-sections on the initial beam polarization has been used to give

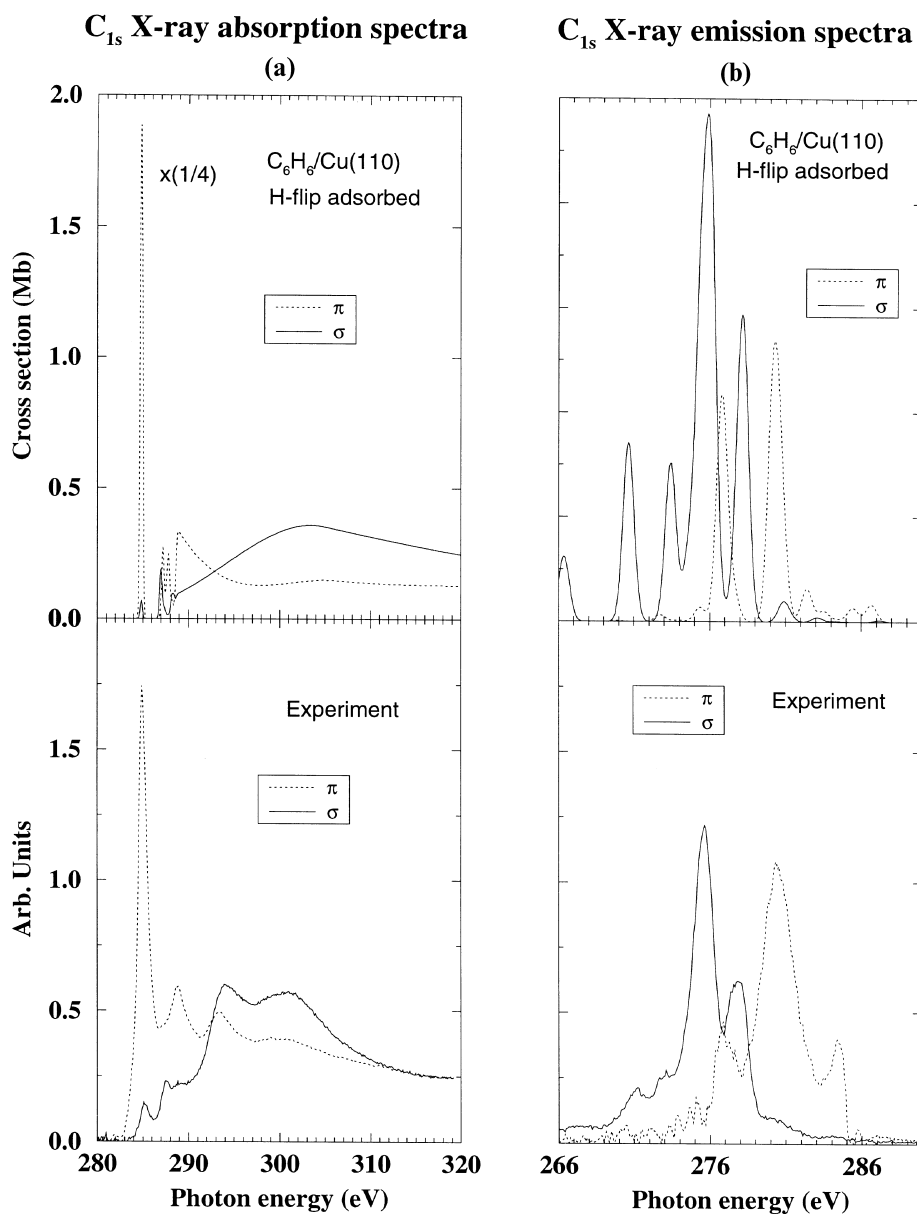


Fig. 4. NEXAFS (a) and XES (b) spectra of  $C_6H_6/Cu_{13}$  for "H-flip" structure compared to the experimental spectra of  $C_6H_6/Cu(110)$  reported in Ref. [32].

a clue on the orientation of benzene when adsorbed on different surfaces, and also on the symmetry assignments of the core excited states. This possibility has been utilized in previous experimental NEXAFS studies, for example, Pt(111) [21],

Mo(110) [34], Ag(110) [35] and Ag(111) [24],  $C_6H_6/Cu(110)$  [32] and  $C_6H_6/Ni(100)$  [32]. Thus from measurements with polarization of the exciting beam orthogonal and parallel to the surface, the  $\pi$  character of the first strong resonance has

been established as well as the  $\sigma$  dominant character of the two continuum resonances. They prove that the benzene molecule basically lies flat on the surface (see also experiments on the Ni(110) [36] and Ni(111) [37] surfaces). However, they also indicate dominant  $\pi$  character for the second discrete band or a  $\pi$ -like shoulder as in the case of  $C_6H_6/Ni(100)$  [32] and  $C_6H_6/Mo(110)$  [34], and some residual character of the first band, seemingly contradicting the assignment for free benzene proposed above. The NEXAFS spectra of  $C_6H_6/Mo(110)$  [34] and  $C_6H_6/Ag(110)$  [35] appear in these respects very similar to the ones of  $C_6H_6/Ni(100)$  and  $C_6H_6/Cu(110)$ , respectively. In these works the spectral changes have been attributed both to the generation of a second  $\pi^*$  state (through molecular  $\pi^*$  and metal d- $\pi$  hybridization), and to the generation of tilted configurations in the adsorption process [35]. Tilting of benzene on the surface has also been advocated based on angularly resolved photoemission measurements of  $C_6H_6$  adsorbed on Cu(110) [38].

From the results described above on boat and H-flip forms, we comment in this subsection some of the assignment issues with regards to free and adsorbed benzene. The presence of the residual  $\sigma$  type intensity already in the distorted *free* benzene (boat or H-flip) means that the presence of such features for adsorbed benzene do not necessarily imply tilting of the molecule. A second comment concerns the appearance of the NEXAFS spectra of H-flip and boat form benzene, which have computed chemisorption energies of 18 and 14 kcal mol<sup>-1</sup>, respectively. We note that simulations of the H-flip, less strongly chemisorbed, form explain the benzene-Cu(110) spectrum well, while the more strongly interacting boat form, with three close-lying resonances, can be used to explain the NEXAFS spectrum for benzene on Ni(100) [32]. The same seems to hold for the  $C_6H_6/Ag(110)$  [35] and  $C_6H_6/Mo(110)$  [34]; the former system shows a second  $\pi$  peak some 4 eV above the first  $\pi^*$  resonance, while benzene chemisorbed on molybdenum shows a broadening of the first  $\pi^*$  resonance just as in the case of chemisorption on Ni(100). As discussed by Liu et al. [34] the reaction and bonding characteristics for Ag(110) and Mo(110) are quite different: for saturation

initial coverages of benzene on Ag(110) the activation energy for desorption is 10 kcal mol<sup>-1</sup>, compared to 22 kcal mol<sup>-1</sup> for benzene on Mo(100) [26, 34]. It is thus tempting to suggest the Mo(110) and Ni(100) NEXAFS features as being a general fingerprint of the more strongly chemisorbed boat-form benzene and the Cu(110) and Ag(110) features as a general fingerprint of the H-flip less strongly adsorbed benzene.

Thirdly, the assignment of the third and fourth main experimental features at 294, respectively, 300–305 eV in the continuum is identical for free and adsorbed, boat or H-flip, forms of benzene. The absence of intensity of the 294 eV structure from the present, near-basis set limit, independent-particle calculations thus provide an indirect support for an assignment of this structure as due to multi-electron excitations. (It is here noteworthy that the polarization selective spectra of Cu(110) [32] also show some  $\pi$  character of this resonance). In the surface adsorbed boat form the  $\sigma^*$  resonance shifts upwards a few eV, as would be anticipated for a significant prolongation of the C–C bondlength, while for H-flip adsorbed benzene it seems identical to free benzene.

Finally, we find the simulations to indicate that both the bond formation and the internal restructuring of the benzene molecule upon adsorption significantly perturb the NEXAFS spectra, distributing  $\pi$  and  $\sigma$  character to parts of the spectra not predicted for free benzene. The fact that neither “planar free” nor “H-flip” free benzene predicts  $\pi$  intensity in the upper discrete region implies that the appearance of these  $\pi$  state(s) in the experimental spectra refers to the actual bonding to the surface. For boat form benzene such structures exist in the free molecule, but are further enhanced in the adsorbed form. Thus the actual bonding to the surface does change the NEXAFS spectrum. As a corollary to that statement one can resolve the mismatch between symmetry assignments of the adsorbed spectra and those of calculations of the free benzene species. This seems to be the situation also for other hydrocarbons, for example, butadiene, for which results from calculations of the free species are at variance with the orientational dependence of the NEXAFS spectra of the corresponding chemisorbed species [6].

### 3.3. XES spectra

#### 3.3.1. XES of free benzene

The XES of free benzene have been firmly assigned both with non-resonant and resonant excitation and are well reproduced by the simulations at a frozen orbital level of theory [39], see

Fig. 5. The six bands observed in the experimental non-resonant spectrum at 280.4, 277.5, 275, 273.7, 270.3 and 266.3 eV can thus be assigned to X-ray transitions involving the  $1e_{1g}$ ,  $3e_{2g}+1a_{2u}$ ,  $3e_{1u}+1b_{2u}+2b_{1u}$ ,  $3a_{1g}$ ,  $2e_{2g}$ ,  $2e_{1u}$  orbitals, respectively, following also the UPS assignments [40,41]. The last two bands are weak because of the  $2s$

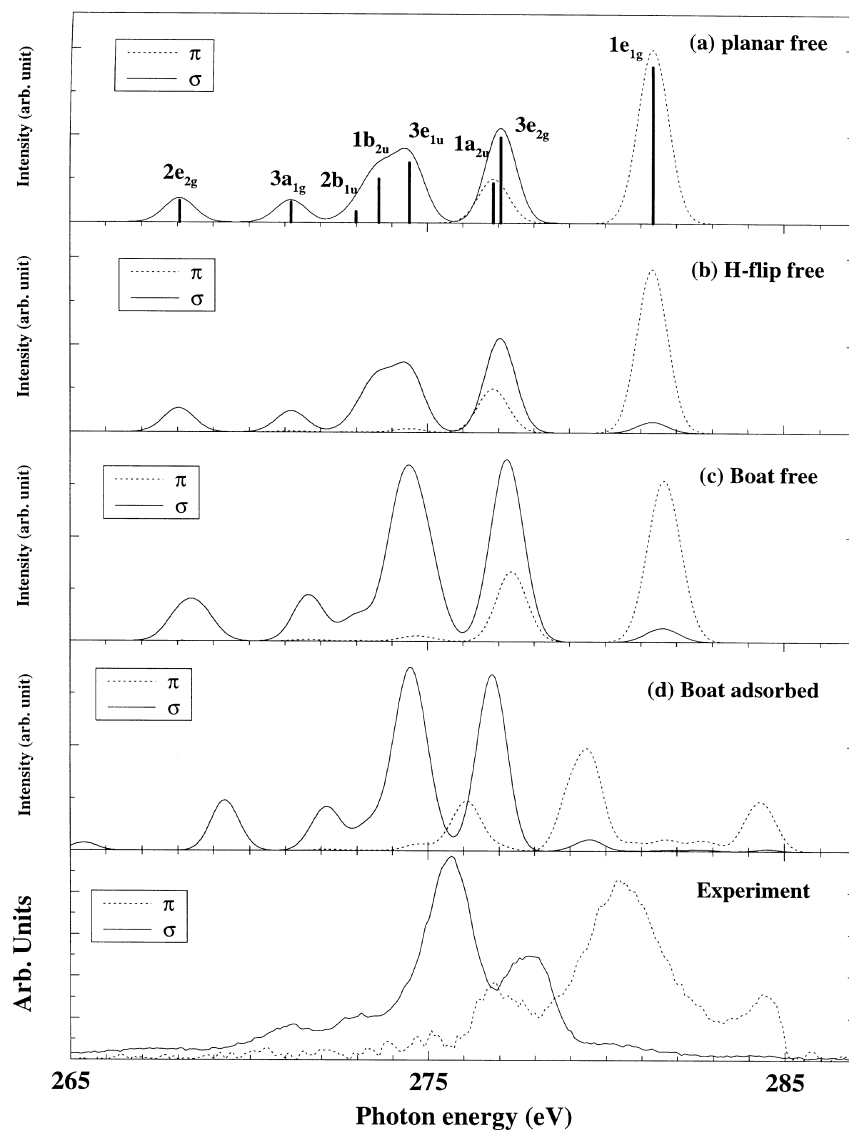


Fig. 5. Simulated XES of benzene at relaxed orbital approximation. Spectral lines are convoluted with gaussians with FWHM = 1.0 eV. (a) Planar free benzene in gas phase geometry. (c) Free benzene with distorted boat form geometry. (d) Surface adsorbed benzene with distorted boat form geometry. The factor of 1.2 for compressing the spectral width has been used [39,58].

character of the corresponding MOs and because of the breakdown of the molecular orbital picture with accompanying correlation state splittings.

In Fig. 5a and c we present the simulated spectra of benzene at the “planar”, “H-flip” and “inverted boat” geometries. We note that surface orthogonal detection of planar benzene reflects orbital emission while surface parallel detection reflects both  $\pi$  and  $\sigma$  orbital emissions. In the case when  $\sigma$ - $\pi$  separability is broken “ $\sigma$ ” and “ $\pi$ ” should be interpreted as directional components of the vector components  $[x, y]$  and  $[z]$ , respectively (“atomic subsymmetries”). The calculations predict a clear to separability of the XES spectrum, save the second structure at 277 eV which is a superposition of the  $3e_{2g}\sigma$  and  $1a_{2u}\pi$  orbital emissions. On a coarse scale the spectral profile is roughly intact when the hydrogens are flipped (Fig. 5b) and when the carbon ring is distorted (Fig. 5c).

### 3.3.2. XES of $C_6H_6/Cu_{13}$

The computed XE spectra for chemisorbed, “boat” and “H-flip”, benzene are shown in Fig. 4dFig. 5. The spectral profiles are similar to those of the gas phase distorted structure on a coarse scale. On a finer scale one can observe effects of degeneracy-lifting and of a slightly deteriorated “ $\sigma$ - $\pi$ ” separability, that is, “ $\pi$ ”-derived emission propagates down while “ $\sigma$ ” orbital emission propagates up in the spectrum. At the energy of the  $1e_{1g}$  HOMO (highest occupied molecular orbital) there is thus some underlying “ $\sigma$ ” emission for the chemisorbed benzene species. Furthermore, high-energy bands appear in the  $\sigma$  and  $\pi$  parts. The most conspicuous difference between free and chemisorbed distorted benzene, is the intensity in the gap between the  $1e_{1g}$  and the  $1e_{2u}$  levels as well as intensity for the  $1e_{2u}$  level itself. One also notes small background  $\sigma$  contributions in this part of the spectrum.

The recently published XES spectra of  $C_6H_6/Cu(110)$  and  $C_6H_6/Ni(100)$  [32] show an extra high-energy feature and a small [larger for Ni(100)]  $\sigma$  tail that reaches towards the Fermi level, see Fig. 4. The experimental comparison indicates that “ $\sigma$ ” bonds participate in the adsorption of benzene. The XE spectra do not seem to

distinguish the two chemisorbed structures as well as the NEXAFS spectra.

The XE spectra so far discussed have all been generated within a frozen orbital picture, that is, no relaxation is included neither for the initial core hole state nor for the final valence hole state. It can be of interest to investigate separately the effects of relaxation of the core hole state, as in the XPS state, or mimicking the resonantly excited process by determining the relaxed core hole state in the presence of the excitation. The XE spectra of the free and chemisorbed distorted benzene are shown in Fig. 6a–f for the cases of frozen orbital-, “relaxed including excitation”-, and relaxed pure core hole spectra.

### 3.3.3. Frozen versus relaxed calculations

With the inclusion of orbital relaxation one obtains a spectrum which differs fairly little in the “bound” part, but which enhances the  $e_{2u}$ -derived transitions ( $e_{2u}$  is the LUMO orbital in free benzene). As seen by comparing Fig. 6a(d) and 6c(f) the primary role of relaxation is to enhance the ratio of  $\pi$  versus  $\sigma$  electron emission, while the internal  $\sigma$  spectrum largely remains intact (note that the spectra are renormalized according to the highest peak). This enhancement is a typical feature of hydrocarbon systems, for which the outermost levels easily develop excitons in the long-chain limit, see Ref. [42]. For the present surface adsorbed system (as also for, for example, the  $\pi^*$ -level of adsorbed CO [8]), an even more conspicuous feature is the enhancement of the screening  $e_{2u}$  level, as further discussed in Section 3.3.5. In the relaxed calculation the initial state is the fully relaxed core-hole state, while for the final valence hole state the frozen ground state orbitals are used in combination with energies from Koopmans’ theorem. The energies are quite accurate for free benzene and should be so also for the chemisorbed species [43]. There may be effects on the intensities from valence hole relaxation, in particular for the chemisorbed system, where additional screening involving substrate levels can be obtained. A problem of explicitly considering each fully relaxed final hole state separately is, however, the necessity to treat the interaction between the resulting non-orthogonal final

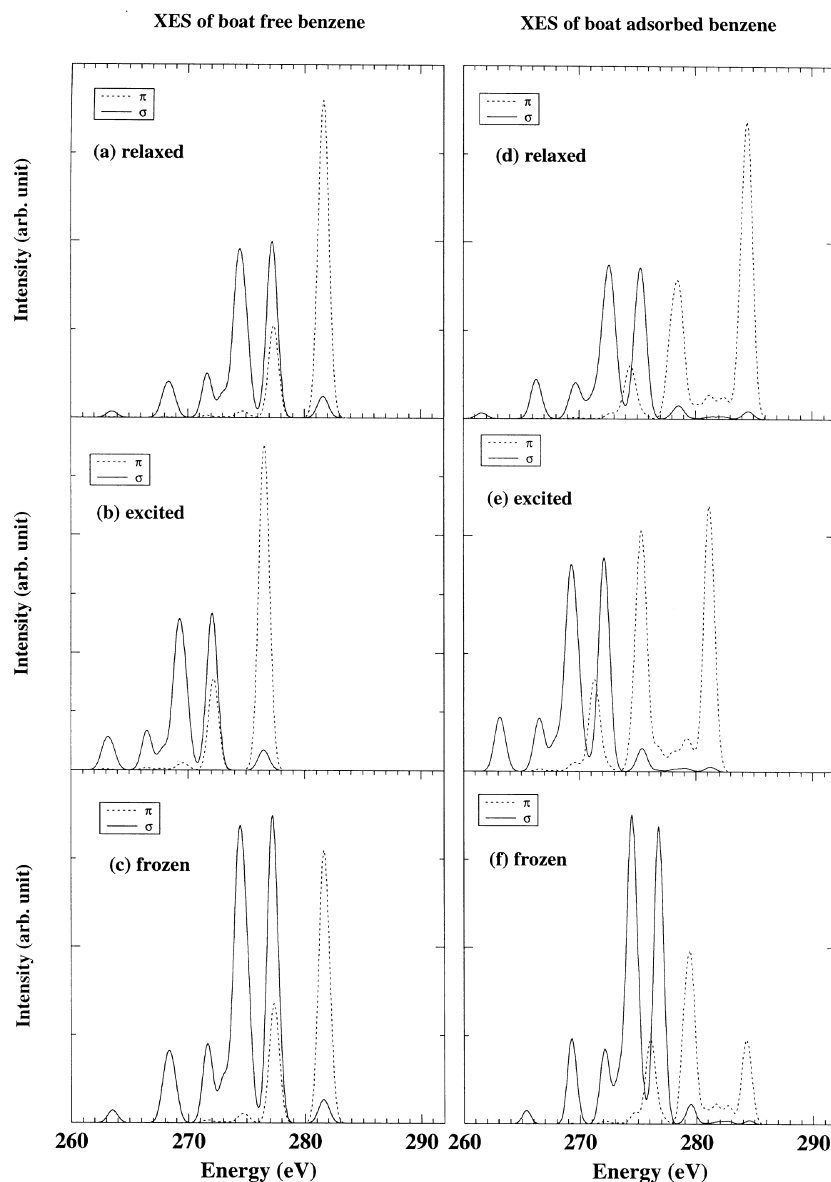


Fig. 6. Simulated XES of gas phase distorted (a–c) and surface adsorbed benzene (d–f) with different treatment of relaxation effects. (a) and (d) fully relaxed core-hole, (b) and (e) fully relaxed core hole in the presence of excitation, (c) and (f) frozen (unrelaxed) core orbitals. Spectral lines are convoluted with gaussians with FWHM=1.0 eV.

states; this problem has not yet been solved within the present implementation.

#### 3.3.4. Possible symmetry selection

A conspicuous feature of RIXS (resonant inelastic X-ray scattering) spectra is the manifestation

of symmetry selection. The “prepared” symmetry of the core excited state leads to symmetry selection in the emission. The prediction – and observation – of forbidden  $e_{1g}$  emission of free benzene upon  $C\ 1s \rightarrow e_{2u}$  absorption serves as a verification of this contention [44]. However, the

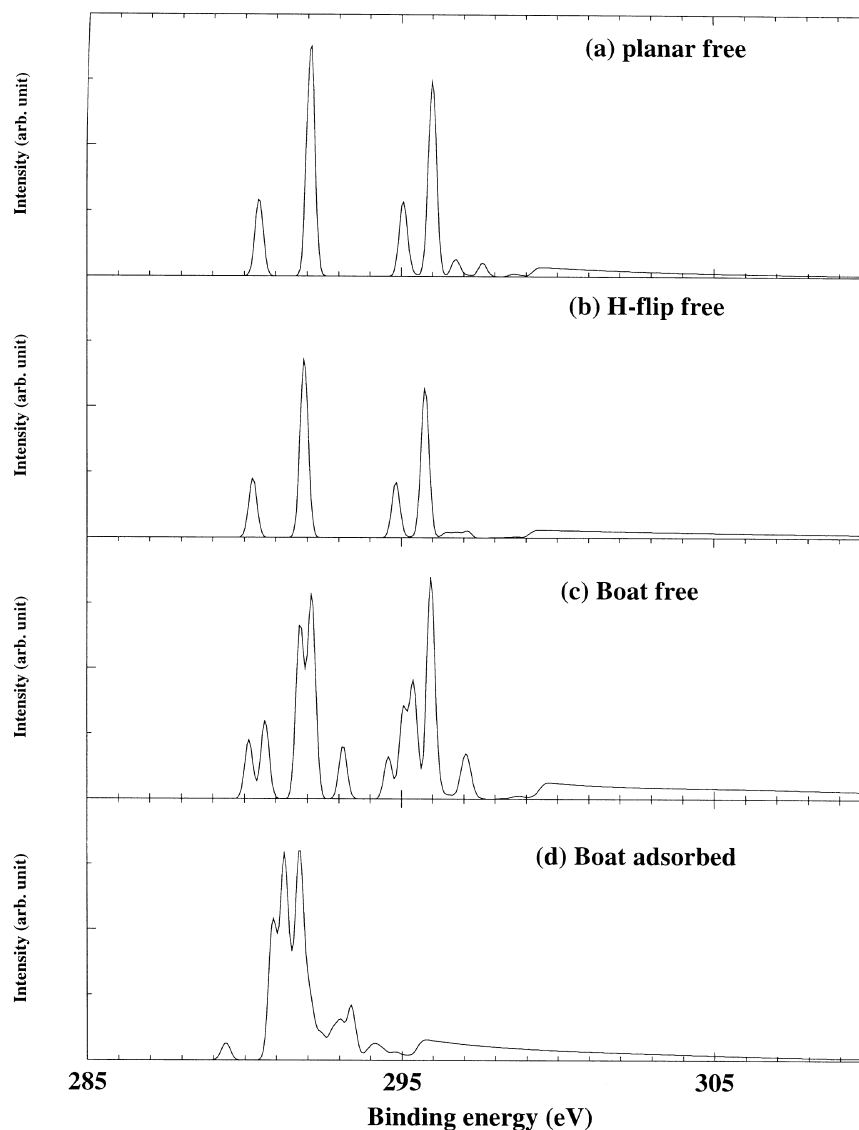


Fig. 7. Simulated XES of gas phase distorted (a–c) and surface adsorbed benzene (d–f) with different treatment of relaxation effects. (a) and (d) fully relaxed core-hole, (b) and (e) fully relaxed core hole in the presence of excitation, (c) and (f) frozen (unrelaxed) core orbitals. Spectral lines are convoluted with gaussians with FWHM=1.0 eV.

C  $1s \rightarrow e_{2u}$  related emission in free benzene also shows symmetry forbidden transitions,  $1a_{2u}$  and  $3e_{2g}$ , as one might expect from the indication that the core excited C  $1s \rightarrow e_{2u}$  state itself is symmetry broken [28,29]. Symmetry selection is sensitively dependent on the excitation frequency (“symmetry restoration by detuning the frequency” [45]), and the benzene spectrum is probably further compli-

cated by Jahn–Teller instability of the final states. In the surface adsorbed case one can anticipate some restoration of the symmetry selectivity as a consequence of channel interference between the chemically shifted core excited states [46]. Comparing with experimental angular resolved  $e_{2u}$  excited spectra [32] it seems actually to be the  $3e_{3g}$  level which bears reminiscence of symmetry

selection for surface adsorbed benzene, rather than the  $e_{1g}$  level as for polymerized or substituted benzene [46,47]. For a complete  $D_{6h}$  group theory analysis of the benzene RIXS spectra involving the first six core excitation resonances we refer to Ref. [44].

### 3.3.5. Resonant versus non-resonant XES spectra

The XES calculations implement a non-resonant X-ray emission model, that is, the spectra are assumed to emanate from an initial bare core hole state. On the other hand the experimental spectra are, primarily for intensity reasons, generated by resonant excitation to the first unoccupied “ $\pi^*$ ” band. In the present model we indeed obtain a signal from the “ $\pi^*$ ” band in the frozen orbital approximation due to the slight population of the  $e_{2u}$  derived level in the ground state; this signal, however, increases quite drastically in the relaxed orbital approximation. Thus in the non-resonant model this level is populated by surface screening rather than by excitation as would be the case in a resonant model. In order to simulate the effect of resonant excitation to some extent we optimized explicitly the core-excited state with a  $\pi^*$  electron present, and computed the (non-resonant) emission spectrum with the so optimized orbitals. The outcome of this procedure was somewhat different for the gas phase species and the surface adsorbed benzene. For the gas phase molecule the relaxed spectra with or without the excited electron have identical appearance (apart from a general energy shift to lower binding energies when the excited electron is included; this seems to concord with results of screening calculations on free molecules using explicitly electron-correlated methods [48]). It seems that all screening of the core hole is accounted for through localization of the  $1e_{1g}$  orbital at the core site in question. For the surface adsorbed benzene it seems that the excited electron and surface-derived states participate strongly in the screening. Comparing spectra 5d and 5e one sees a large effect on the  $\pi$ -state at the Fermi level from removal of the excited electron, which clearly indicates both that the excitation itself can provide screening and that contributions from charge-transfer processes are of importance. It should be remembered, however, that in the calculations the

screening of the final valence hole has not been accounted for. In Figs. 5 and 6 only relative intensities within a given spectrum are considered; a comparison of intensities between the different spectra requires in principle also the computation of the fluorescence yields (and Auger rates).

There is a discrepancy remaining, namely that referring to the emission intensity of the  $\pi^*$  level itself; the screening intensity obtained by the relaxed non-resonant model seemingly overestimates this intensity, an observation in common with for example, results for CO on copper [8]. Apart from the shortcomings in the modelling of the  $\pi^*$  emission, one must here account for the quite different natures of inelastic and elastic scattering processes, as one can expect from the experience with free atoms and molecules. The investigations in the field of *elastic* RXS (REXS, or anomalous elastic X-ray scattering) have primarily focussed on X-ray diffraction, while, in contrast to the inelastic case, the fine-structure of cross-sections near the ionization threshold has been little attended [49]. The inelastic and elastic processes differ in a number of ways, primarily by the off-resonant so-called form factor and the contributions from scattering through higher-lying intermediate states in the elastic case. One can also add the problem of self-absorption of the elastic signal and the fact that the  $\pi^*$  electron *might* delocalize over the surface on a time scale of the duration of the REXS process, thereby depleting the elastic signal. Considering the lack of general theory for elastic scattering on surface adsorbates, we refrain from pushing our computational model further.

## 3.4. XPS shake-up spectra

### 3.4.1. Free benzene shake-up

An obvious problem for the interpretation of shake-up of surface adsorbed benzene is the lack of consensus in the interpretation of the shake-up spectrum of free benzene. In fact the consensus is restricted to the dominant role played by excitations within the  $\pi$  manifold of orbitals. Different methods so far employed indicate different excitation patterns for describing the salient four-peak shake structure of this molecule. The presently

maintained interpretation of the shake-up spectrum in terms of singlet optical excitations in the  $Z+1$  potential disagrees with corresponding calculations with correctly spin-adapted wave functions (using otherwise identical configurational spaces). However, also the STEX results, although using correctly spin-adapted wave functions, differ to some extent from MCSCF/CI wave function results [50]. Apart from including higher excitations (for the two higher bands), the latter methods also couple the two (parent singlet and triplet spin-coupled) functions relevant for the purely single-excitation low-energy bands. The STEX wave function in the direct SCF implementation, excludes higher-order excitations describing inter-channel interactions, but reaches the full intrachannel limit in an almost completely saturated basis set.

In the present work we take a pragmatic approach and note that the STEX results recapitulate the four-peak structure in the shake spectrum of free benzene sufficiently well to motivate a study of the chemisorbed system (here in the boat-form, Fig. 7). The STEX hole-coupling calculations thus provide an interpretation of the salient four-peak structure in terms of singlet and triplet parent hole coupled  $2b_1-3b_1$  and  $1b_1-3b_1$  excitations, using symmetry broken  $C_{2v}$  notation.

#### 3.4.2. $C_6H_6/Cu_{13}$ shake-up

It is relevant to compare the appearance of the shake spectrum for  $C_6H_6/Cu_{13}$ , Fig. 8, with features generally encountered in surface adsorbate shake spectra, namely first a region with (generally weak) low-energy excitations localized to the cluster, then an intermediate region with (generally strong) cluster-to-adsorbate charge transfer excitations, and finally a high energy region, overlapping the shake-off continua, which contains transitions which can be described as intramolecular (internal adsorbate) orbital excitations. The first type of low-lying shake transitions appear only as an asymmetrical broadening of the main core photoelectron lines, while the second charge transfer region crucially depends on the strength of chemisorption [51], and might be so strong that the distinction between “main” and “satellite” peaks is no longer obvious. The third type is

embedded in the continua of very many shake channels, and is considerably weakened because of that. Benzene is somewhat special in that the  $\pi-\pi$  transitions are of low energy already for the free molecule, comparable to charge transfer excitation energies. We also find, that the salient structures at 4–6 eV in the spectrum of the chemisorbed molecule are dominated by internal benzene excitations, rather than by charge-transfer transitions as predicted for other related systems (e.g. in the corresponding  $CO/Cu_{13}$  cluster [52]). As for free benzene, few channels are active, and in each such channel there are only few excitations that provide intensity to the shake spectrum. The two chemically shifted spectra for free “boat-benzene” appear to be similar, save for an extra peak in the C3 spectrum, which can be interpreted as shake-up to the upper split  $e_{2u}$  component in that case. The difference between the two spectra is obviously larger for the cluster. We also note a weak, low-energy feature which can be assigned as due to a delocalized, off-site excitation in the cluster, which thus can be interpreted as a reminiscence of the hole-pair excitations [53] typical for describing the asymmetrization of the core photoelectron lines in solids.

## 4. Summary

The present work is an example of theoretical modelling of geometric and electronic structures of surface adsorbates that increasingly has been employed in the context of X-ray spectroscopies. Such simulations open ways to obtain special relationships between the structures and various spectral features and thereby the possibility to validate or invalidate the structures actually predicted, either by other simulations or by experimental techniques. The use of X-ray spectroscopies has in this respect been much revived owing to the possibility to use monochromatized and polarized synchrotron radiation in a broad range of X-ray energies. This has brought about new means of probing adsorbate orientation as well as the electronic structures that are local to the atomic sites involved in the X-ray process. Unlike valence band spectroscopies, for which one obtains signals

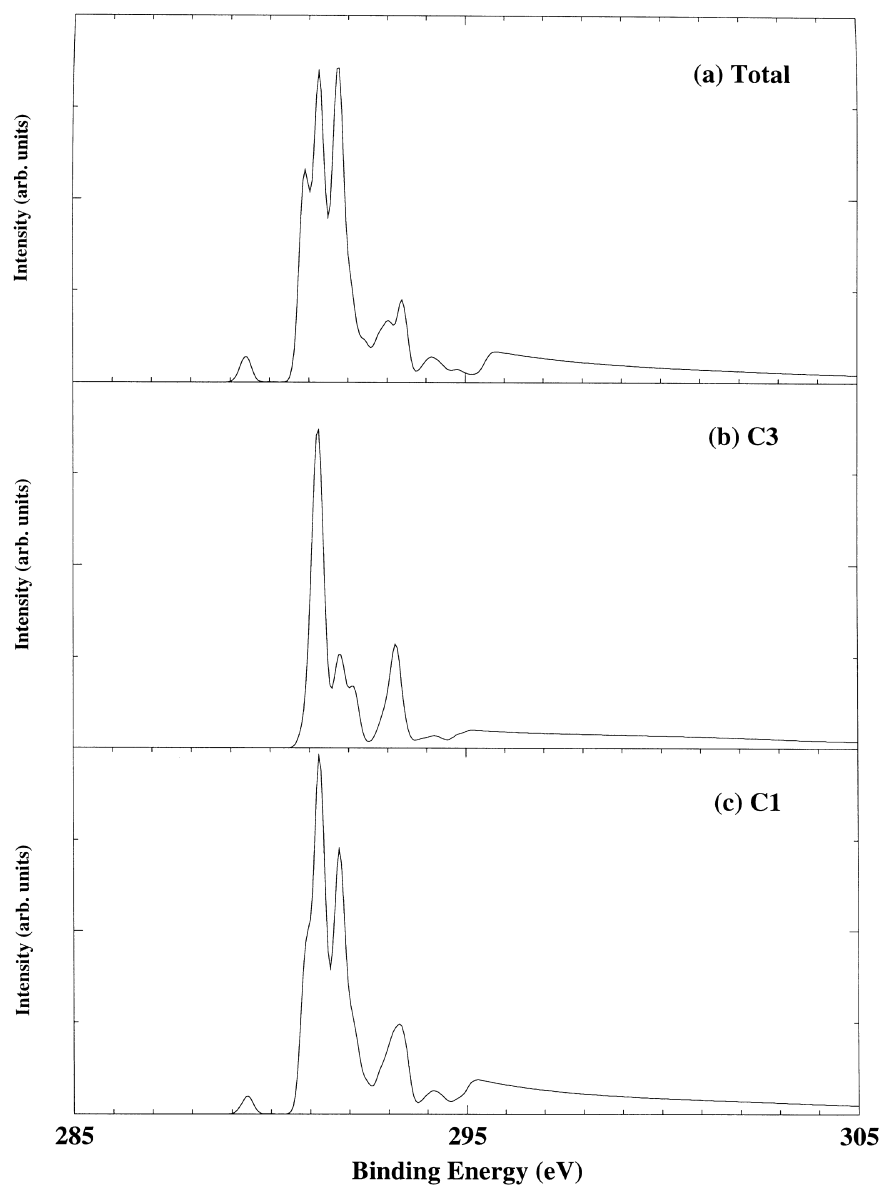


Fig. 8. Simulated shake-up spectra of surface adsorbed benzene. Spectral lines are convoluted with gaussians with FWHM=0.3 eV. (a) Total spectrum, (b) C1 spectrum, (c) C3 spectrum.

that represent the delocalized states, the X-ray signals indeed reflect the part of the electronic structure that is localized to the adsorbate, and can provide information of the bonding of different elements or of different chemically shifted species in the adsorbate. The support from simulations to

extract the proper information is indispensable in many such cases.

By choosing a model for a prototype surface adsorbate we have shown that restructuring of the adsorbate upon bonding can lead to significant and characteristic changes in X-ray spectra – XES,

NEXAFS and shake-up. Geometry optimization of  $C_6H_6$  on a  $Cu_{13}$  cluster model of the Cu(110) surface has led to two optimum adsorbate conformations, one with the carbon ring bent in an inverted boat-like form and with the hydrogen atoms flipping upwards [3], and one in which the carbon ring planarity is maintained but with the hydrogens bending. In the first conformation the bending of the carbon plane is  $7.4^\circ$ , with four C–C bonds prolonged by 0.05 Å, while the top-plane carbon and hydrogen atoms keep their bond lengths intact. Such changes have been anticipated but not accepted as a statistically significant fact [4]. In the second structure the C–C bond length is only slightly (0.02–0.03 Å) elongated compared to gas phase, but with the C–H bending angle for four hydrogens similar to that for the boat structure; two hydrogens show a smaller bending angle.

The difference in the predicted X-ray spectra referring to the two different molecular states of the benzene molecule involved in the interaction with the substrate and the  $\sigma$ – $\pi$  symmetry-breaking manifested in the orientational dependence of these spectra should be significant enough to make it possible to test structural changes upon adsorption by actual X-ray measurements. This also puts the picture of bond-prepared adsorbate structures [3] to test, where in the present case of benzene adsorption on Cu(110) the excited quinoid triplet state is predicted to lead to the strongest interaction with the substrate.

The most intriguing observation in the experimental NEXAFS spectra is the extra “ $\pi$ ”-symmetry feature above the first resonance. The analysis of this feature results in different assignments depending on the assumed structure; in the inverted boat case as the splitting of the  $e_{2u}$  level from the distortion of the benzene ring, while the second “H-flip” geometry implies this spectral structure as due to additional  $\pi$ -contributions emanating from the surface bonding. The comparison with the available NEXAFS measurement of benzene on a copper (110) surface favours the “H-flip” geometry, and thus the latter assignment for this particular case. It was noted that the corresponding spectrum for  $C_6H_6/Ni(100)$  [32] resembles more closely that computed for the inverted boat structure. Other NEXAFS spectra of benzene

show similar patterns [26], for instance Ag(110) resembles Cu(110) and Mo(110) resembles Ni(100), and it was argued that the extra well separated  $\pi$  feature can be used as a fingerprint for the H-flip—weakly adsorbed—form of benzene, while a feature close to the main peak fingerprints the boat—more strongly adsorbed—form of benzene.

The results for XES verify the NEXAFS results in that a breaking of  $\sigma$ – $\pi$  separability is evident in the simulated spectra. For both adsorbate structures  $\sigma$  intensity propagates upwards in the spectrum, indicating a weak participation in the surface bonding. The comparison is obtained at a frozen orbital level of approximation, and thus reflects the actual (local) electronic structure. The relaxed orbital picture gave some smaller “corrections”, which however, not necessarily seemed to improve the experimental comparison. A conspicuous feature is the drastic increase of the signal from the  $\pi^*$  band, referring to the cluster to benzene charge transfer screening of the core hole, and which seemingly contradicts observations for the resonantly generated spectrum.

The changes of the shake-up spectrum of benzene upon adsorption are predicted to be comparatively small, and the spectrum seems to retain the molecular signatures quite well. Shake-up spectroscopy seems, however, to be less suitable as a diagnostic tool for internal restructuring of adsorbates than XES and NEXAFS for several reasons; the complexity of the spectral features, the difficulty of simulating even the free system, and that the monopole selection rules can not match the simple local selection-, dipole- or polarization rules for X-ray radiative spectra as aid for the analysis.

In the particular case of benzene adsorption on Cu(110) the comparison with the experimental data indicates that the state studied experimentally does not correspond to the one obtained from the calculations as the most strongly chemisorbed. However, the picture of the bondformation as an explicit involvement of the triplet excited state also implies the possible existence of barriers to the formation of specific states on the surface. In fact, such barriers have been predicted theoretically for ethylene on Cu(111) [54] and for acetylene on the same substrate [55]. In the present case, con-

sidering the large excitation energy involved and the repulsion against the sp-band of the copper substrate [55], it is probable that chemisorption at low temperature (80 K), such as in the recent investigation by Nilsson and coworkers [32], should lead to chemisorption into a precursor state rather than the more strongly chemisorbed and strongly distorted species found in the calculations. In fact, when benzene is formed from cyclomerization of three acetylenes on Cu(110) a higher desorption temperature (325 K) than for the chemisorbed species (280 K) was found [56]; this was taken to indicate that the evolution of benzene was reaction controlled rather than desorption controlled in this case. However, early studies of this reaction [57] indicated the presence of benzene after heating to 280 K and cooling back down. From this it seems not impossible that benzene, when formed through the reaction at the Cu(110) surface, could be formed as a more strongly bound species, that is, avoiding the barrier through a different mechanism to form the adsorbed species. The present work can then be used as a fingerprint to help identify or exclude this species as a result of this reaction.

### Acknowledgements

The authors acknowledge the authors of Ref. [32] for useful discussions and for providing their NEXAFS and XES spectra of C<sub>6</sub>H<sub>6</sub>/Cu(110) prior to their own publication. Y. Luo greatly appreciates the financial support provided by Hellmuth Hertz Foundation. This work was supported by the Swedish Natural Science Research Council.

### References

- [1] M.J.S. Dewar, Bull. Soc. Chim. France 18 (1951) 79.
- [2] J. Chatt, L.A. Duncanson, J. Chem. Soc. (1953) 2939.
- [3] L. Triguero, L.G.M. Pettersson, B. Minaev, H. Ågren. to be published.
- [4] D.P. Woodruff, in: R.M. Lambert, G. Pacchioni (Eds), Chemisorption and reactivity of Supported Clusters and Thin Films, Towards an Understanding of Microscopic Processes in Catalysis, Kluwer, Dordrecht, 1997, p. 193.
- [5] H. Ågren, V. Carravetta, O. Vahtras, L.G.M. Pettersson, Chem. Phys. Lett. 222 (1994) 75.
- [6] V. Carravetta, H. Ågren, L.G.M. Pettersson, O. Vahtras, J. Chem. Phys. 102 (1995) 5589.
- [7] L.G.M. Pettersson, H. Ågren, O. Vahtras, V. Carravetta, J. Chem. Phys. 103 (1995) 8713.
- [8] L.G.M. Pettersson, H. Ågren, O. Vahtras, V. Carravetta, Surf. Sci. 365 (1996) 581.
- [9] J.P. Perdew, Y. Wang, Phys. Rev. B 33 (1986) 8800.
- [10] J.P. Perdew, Phys. Rev. B 34 (1986) 7406.
- [11] A. Mattsson, I. Panas, P. Siegbahn, U. Wahlgren, H. Åkeby, Phys. Rev. B 36 (1987) 7389.
- [12] U. Wahlgren, P.E.M. Siegbahn, in: D. Salahub (Ed.), Metal–ligand interactions: from atoms, to clusters, to surfaces. Kluwer, Dordrecht, 1991.
- [13] R.A. Kendall, T.H. Dunning, Jr., R.J. Harrison, J. Chem. Phys. 96 (1992) 6796.
- [14] J. Almlöf, K. Faegri, Jr., K. Korsell, J. Comput. Chem. 3 (1982) 385.
- [15] L.G.M. Pettersson, H. Ågren, B.L. Schürmann, A. Lippitz, W.E.S. Unger, Int. J. Quant. Chem. 63 (1997) 749.
- [16] A. St-Amant, D.R. Salahub, Chem. Phys. Lett. 169 (1990) 387.
- [17] D.R. Salahub, R. Fournier, P. Mlynarski, I. Papai, A. St-Amant, J. Ushio, in: J. Labanowski, J. Andzelm, (Eds.), Density Functional Methods in Chemistry, Springer, New York, 1991, p. 77; A. St-Amant, Ph. D. Thesis, Université de Montréal, 1992. The present version of the program has been substantially modified by L.G.M. Pettersson.
- [18] A.J.H. Wachters, J. Chem. Phys. 52 (1970) 1033.
- [19] G. Held, M.P. Bessent, S. Titmuss, D.A. King, J. Chem. Phys. 105 (1996) 11305.
- [20] A.P. Hitchcock, M. Pocock, C.E. Brion, M.S. Banna, D.C. Frost, J.A. MacDowell, B. Wallbank, J. Electron Spectrosc. Relat. Phenom. 13 (1978) 345.
- [21] J.A. Horsley, J. Stöhr, A.P. Hitchcock, D.A. Newbury, A.L. Johnson, F. Sette, J. Chem. Phys. 83 (1985) 6099.
- [22] P. Yannoulis, R. Dudde, K.H. Frank, E.E. Koch, Surf. Sci. 189/190 (1987) 519.
- [23] W.H.E. Schwarz, T.C. Chang, U. Seeger, K.H. Hwand, Chem. Phys. 117 (1987) 73.
- [24] T. Yokoyama, K. Seki, I. Morisada, K. Edamatsu, T. Ohta, Phys. Scripta 41 (1990) 189.
- [25] H. Ågren, V. Carravetta, O. Vahtras, Chem. Phys. 195 (1995) 47.
- [26] J. Stöhr, NEXAFS Spectroscopy, Springer Verlag, Berlin, 1992.
- [27] S. Svensson et al., private communication.
- [28] Y. Ma, F. Sette, G. Meigs, S. Modesti, C.T. Chen, Phys. Rev. Lett. 63 (1989) 2044.
- [29] P. Norman, H. Ågren, THEOCHEM 401 (1997) 107.
- [30] O. Plachkevtych, L. Yang, O. Vahtras, H. Ågren, L.G.M. Pettersson, Chem. Phys. 222 (1997) 125.
- [31] J.T. Francis, A.P. Hitchcock, J. Phys. Chem. 96 (1992) 6598.
- [32] A. Nilsson, N. Wassdahl, M. Weinelt, O. Karis, T. Wiell,

- P. Bennich, J. Hasselström, A. Fölich, J. Stöhr, M. Samant. to be published.
- [33] C. Mainka, P.S. Bagus, A. Schertel, T. Strunskus, M. Grunze, C. Wöll, Surf. Sci. 341 (1995) L1055.
- [34] A.C. Liu, J. Stöhr, C.M. Friend, R.J. Madix, Surf. Sci. 235 (1988) 107.
- [35] A.C. Liu, C.M. Friend, J. Stöhr, Surf. Sci. 236 (1990) L439.
- [36] W. Huber, M. Weinelt, P. Zebish, H.P. Steinrück, Surf. Sci. 253 (1991) 72.
- [37] W. Huber, H.P. Steinrück, H. Pache, D. Menzel, Surf. Sci. 217 (1989) 103.
- [38] J.R. Lomas, C.J. Baddeley, M.S. Tikhov, R.M. Lambert, Chem. Phys. Lett. 263 (1996) 591.
- [39] P. Skytt, J.H. Guo, N. Wassdahl, J. Nordgren, Y. Luo, H. Ågren. Phys. Rev. A 52 (1995) 3572.
- [40] L. Karlsson, L. Mattsson, R. Jadrny, T. Bergmark, K. Siegbahn, Physica Scripta 14 (1976) 7230.
- [41] L.S. Cederbaum, W. Domcke, J. Schirmer, W. von Niessen, G.H.F. Diercksen, W.P. Kraemer, J. Chem. Phys. 69 (1978) 1591.
- [42] F. Gel'mukhanov, L. Yang, H. Ågren, J. Chem. Phys. 105 (1996) 5224.
- [43] J.-L. Pascual, L.G.M. Pettersson, H. Ågren, Phys. Rev. B 56 (1997) 7716.
- [44] Y. Luo, H. Ågren, F. Gel'mukhanov, J. Phys. B At. Mol. Phys. 27 (1994) 4169.
- [45] A. Cesar, F. Gel'mukhanov, Y. Luo, H. Ågren, P. Skytt, P. Glans, P. Guo, K. Gunnelin, J. Nordgren, J. Chem. Phys. 106 (1997) 3439.
- [46] Y. Luo, H. Ågren, J.H. Guo, P. Skytt, N. Wassdahl, J. Nordgren, Phys. Rev. A 52 (1995) 3720.
- [47] J.H. Guo, M. Magnuson, C. Sæthe, J. Nordgren, L. Yang, Y. Luo, H. Ågren, K.Z. Xing, N. Johansson, M.R. Salaneck, W.J. Feast, J. Chem. Phys. 108 (1998) 5990.
- [48] H. Ågren, Y. Luo, F. Gel'mukhanov, H.J.Aa. Jensen, J. Electron. Spectrosc. 82 (1996) 125.
- [49] R.H. Pratt, L. Kissel Jr., P.M. Bergstrom, in: G. Materlik, C.J. Sparks, K. Fischer (Eds.), Resonant Anomalous X-Ray Scattering. Theory and Applications, North-Holland, Amsterdam, 1994, p. 9.
- [50] H. Ågren. Unpublished.
- [51] H. Tillborg, A. Nilsson, N. Mårtensson, J. Electron Spectros. Relat. Phenom. 62 (1993) 73.
- [52] H. Ågren, V. Carravetta, L.G.M. Pettersson, O. Vahtras, Phys. Rev. B 53 (1996) 16074.
- [53] S. Doniach, M. Sunjic, J. Phys. C 3 (1970) 285.
- [54] A. Michalak, M. Witko, K. Hermann, J. Molec. Catal. A 119 (1997) 213.
- [55] A. Clotet, G. Pacchioni, Surf. Sci. 346 (1996) 91.
- [56] J.R. Lomas, C.J. Baddeley, M.S. Tikhov, R.M. Lambert, Langmuir 11 (1995) 3048.
- [57] N.A. Avery, J. Am. Chem. Soc. 107 (1985) 6711.
- [58] E. Ort, J.L. Bredas, J. Chem. Phys. 89 (1988) 1009.